



HAL
open science

X-band compact dual circularly polarized isoflux antenna for nanosatellite applications

Eric Arnaud, Cyrille Menudier, Jamil Fouany, T Monediere, M Thevenot

► **To cite this version:**

Eric Arnaud, Cyrille Menudier, Jamil Fouany, T Monediere, M Thevenot. X-band compact dual circularly polarized isoflux antenna for nanosatellite applications. *International Journal of Microwave and Wireless Technologies*, 2017, pp.1 - 8. <10.1017/S1759078716001410>. <hal-01431624>

HAL Id: hal-01431624

<https://unilim.hal.science/hal-01431624v1>

Submitted on 11 Jan 2017

HAL is a multi-disciplinary open access archive for the deposit and dissemination of scientific research documents, whether they are published or not. The documents may come from teaching and research institutions in France or abroad, or from public or private research centers.

L'archive ouverte pluridisciplinaire **HAL**, est destinée au dépôt et à la diffusion de documents scientifiques de niveau recherche, publiés ou non, émanant des établissements d'enseignement et de recherche français ou étrangers, des laboratoires publics ou privés.



HAL Authorization

X-band Compact Dual Circularly Polarized Isoflux Antenna for nanosatellite applications

E. Arnaud¹, C. Menudier¹, J. Fouany¹, T. Monediere¹, M. Thevenot¹

¹ XLIM – CNRS, 123 Avenue Albert Thomas, 87060 Limoges Cedex, France.

Abstract— This paper presents an original solution to design a compact dual circularly polarized isoflux antenna (DCPIA) for nanosatellite applications. This kind of antenna has been previously designed in our laboratory, for a single circular polarization. This antenna is composed of a dual circularly polarized feed and a choke horn antenna. This feed is a cross-shaped slot in the ground plane which provides coupling between a patch and a ring microstrip line with two ports. It is located at the centre of a choke horn antenna. The simulated antenna presents an axial ratio (AR) lower than 3 dB and a realized gain (RG) close to 0 dB over a 400 MHz bandwidth (8.0-8.4GHz) at the limit of coverage (LOC), i.e. 65° whatever the azimuth angle (φ) and the port. A 20 dB matching for each port and 13 dB isolation characteristics between the two ports have been achieved on this bandwidth. It has been realized and successfully measured.

Keywords: Nanosatellite application, dual circular polarization, compact choke horn, patch antenna, isoflux radiation pattern.

Corresponding author: E. ARNAUD; eric.arnaud@xlim.fr

I. INTRODUCTION

The requests in high data rate for future nanosatellite missions are incompatible with a telemetry application in VHF or S bands contrary to the X-band. The future antennas will have to present both isoflux radiation pattern and circular polarization (CP). Unfortunately, these two characteristics are often discordant. Several solutions have been previously designed by our laboratory. A trade-off between isoflux pattern quality and antenna size was made in [1]-[3]. Whatever the design, the circular polarization was limited to a single polarization. The main goal of this study is to design a dual circularly polarized isoflux antenna for nanosatellite applications. The simultaneous use of this dual circular polarization will increase the data rate. This antenna will be positioned above a 3U nanosatellite platform (100 x 100 x 300 mm³). Table I presents the antenna performances targets. They are set as objectives but not as definitive specifications. Usually, the choke horn antenna is a good way to perform an isoflux radiation pattern [4]-[8]. Without considering their dimensions, a dual circularly polarization and a good isolation between ports are ordinarily obtained using a

septum and an orthomode transducer [9]-[10]. Unfortunately, their physical size is not compliant with a nanosatellite application.

Planar solutions such as an array of patches [11]-[16] are interesting but they suffer from important dimensions and they require a complex feeding network. The proposed original solution is the association between a patch, used as feed, and a choke horn antenna which is based on [1]. The first one provides the dual circular polarization while the latter allows realizing the isoflux radiation pattern.

Several authors have already conceived dual circularly polarized with patch antennas. Some of them [17]-[20] used active components such as PIN diodes to create CP. This solution requires one or several DC bias control. It is not able to do the simultaneous polarization. Some other solutions exploit the even and odd modes in a coplanar waveguide transmission line or use a branch line coupler to create CP [21]-[26]. All these designs limit the antenna miniaturization and the realization easiness. Therefore, in this work the initial feed is based on another solution proposed by Aloni and Zhang [27]-[28]. It is made of a cross-shaped slot in a ground plane which provides a coupling between a patch and a single ring microstrip line. This paper is organized as follows. Section II is a brief reminder of the compact choke horn antenna. Section III describes the feed optimization (using CST Microwave Studio) to reach the desired antenna characteristics over the entire frequency band. This Section also deals with the association with the compact choke horn. The comparison between retro-simulations and measurements is presented in section IV. Finally, a conclusion is given.

TABLE I: ANTENNA PERFORMANCES TARGET

Parameter	specification
Frequency band (GHz)	8.0 - 8.4
Return loss (dB)	< -20
Isolation between ports (dB)	< -20
Polarization	RHCP and LHCP
Limit of coverage (LOC)	65°
Minimum gain at LOC (dB)	0
Pattern shape	Isoflux pattern
Maximum AR(dB) at LOC	3
Maximum antenna dimensions	90 mm of diameter and 8 mm of height above platform

II. Reminder on the compact horn antenna

The already studied design for the choke horn antenna [1] is reminded in Fig. 1. The radiation patterns present an isoflux shape over the whole frequency band but the maximum gain is

obtained for an elevation angle $\theta_{gm} = 35^\circ$ instead of the expected LOC when the mechanical constraints are taken into account. The antenna radiates a mono circular polarization with an AR almost lower than 3 dB at the LOC whatever the azimuth angle (φ). The work in this paper aims to improve this design in order to conceive a dual circularly polarized antenna.

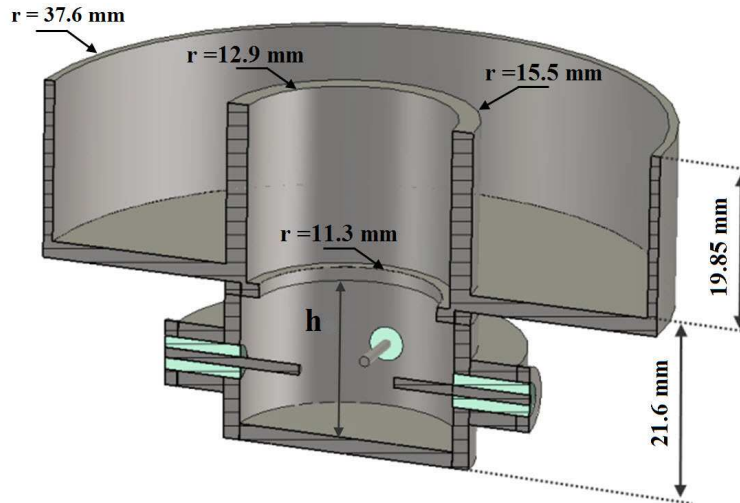


Fig. 1. Definition of the compact choke horn antenna

III. Antenna description

A) Description of the structure

DCPIA (Fig. 2) is obtained by the addition of a dual circularly polarized patch feed (DCPPF) placed on the choke horn aperture (grayed area). The patch replaces the radiating aperture achieved by the waveguide of the antenna designed in [1]. Note that the dimensions of this horn have not been changed except the choke height. Indeed, the patch is excited at the center of the antenna and its radiating pattern is transformed by the interaction with the choke, i.e. by reducing this field at the center of the aperture. To provide a null of the aperture field, the radial position and the height of the choke ring are optimized. This optimization depends to the amplitude of the feed aperture field at the center. Since this parameter is similar between the patch and the radiating aperture, the optimization made in [1] remains correct. On the other hand, the choke height is not uniform ($h_1 < h_2 = 19.85$ mm) to have a RG greater than 0 dB at the LOC whatever the frequency. Notice that one of the aforementioned value is still identical to the design in [1]. The set is inserted into the 3U platform which is simulated as a perfect electric conductor cube but only with a height of 30 mm to reduce the simulation time.

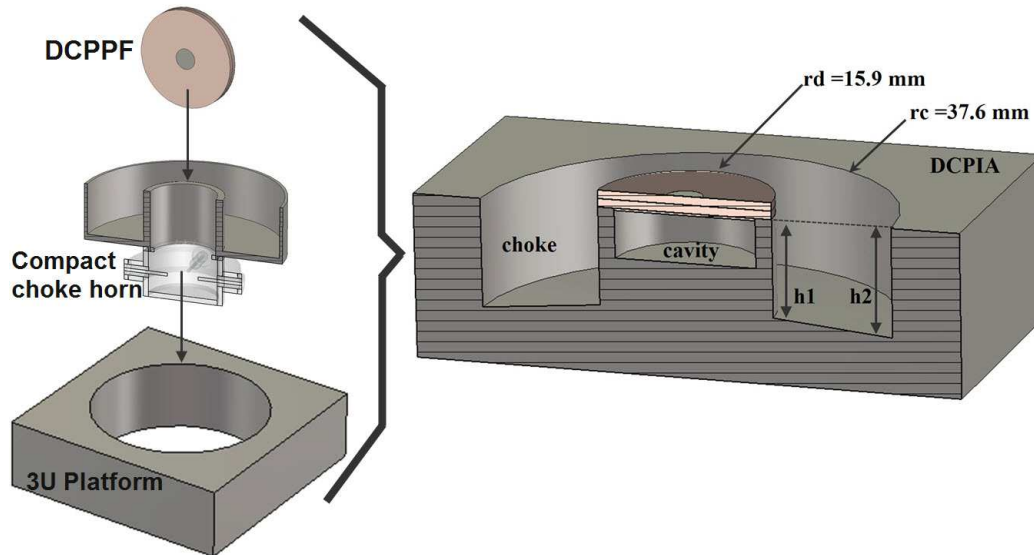


Fig. 2. DCPIA mechanical assembly

The first step towards the goal is to find the best way to realize the feed of DCPIA (Fig. 3).

B) DCPPF design

The feeding part of this antenna is obtained using a cross-shaped slot and a 50Ω ring microstrip line ($wl = 0.91 \text{ mm}$) respectively etched on the top and bottom of the Duroid 4003C laminate (substrate 1). The circular polarization is obtained by a sequential phase feed of the slot ($L_f = 7.4 \text{ mm}$, $l_{af} = 0.5 \text{ mm}$). Port1 produces a left circular polarization (LHCP) while Port2 creates a right circular polarization (RHCP). It is necessary that the microstrip line length between each slot branch corresponds to a 90° phase difference, i.e. a quarter of the guided wavelength (Fig. 4.a). The radiating patch part of the antenna is made of two stacked patches. The lowest one is printed on a Duroid 4003C laminate (substrate 3). It includes two circular-shaped notches to improve the LOC AR whatever the azimuth angle (φ). The upper patch which is etched on the top of this same substrate is useful for increasing the isolation bandwidth between both circularly polarized waves. Last substrate (substrate 2) without metallization is identical to the substrate 3 and it is sandwiched between the two other substrates. Firstly, this structure has been optimized in order to obtain the best electromagnetic performances taking into account mechanical constraints. Secondly, the whole antenna has been simulated on the 3U platform. The electromagnetic characteristics are almost identical except the radiation pattern (conventional patch radiation pattern to isoflux radiation pattern). A cylindrical cavity below the patch feed is created to reduce the DCPIA back radiation due to the slot [29].

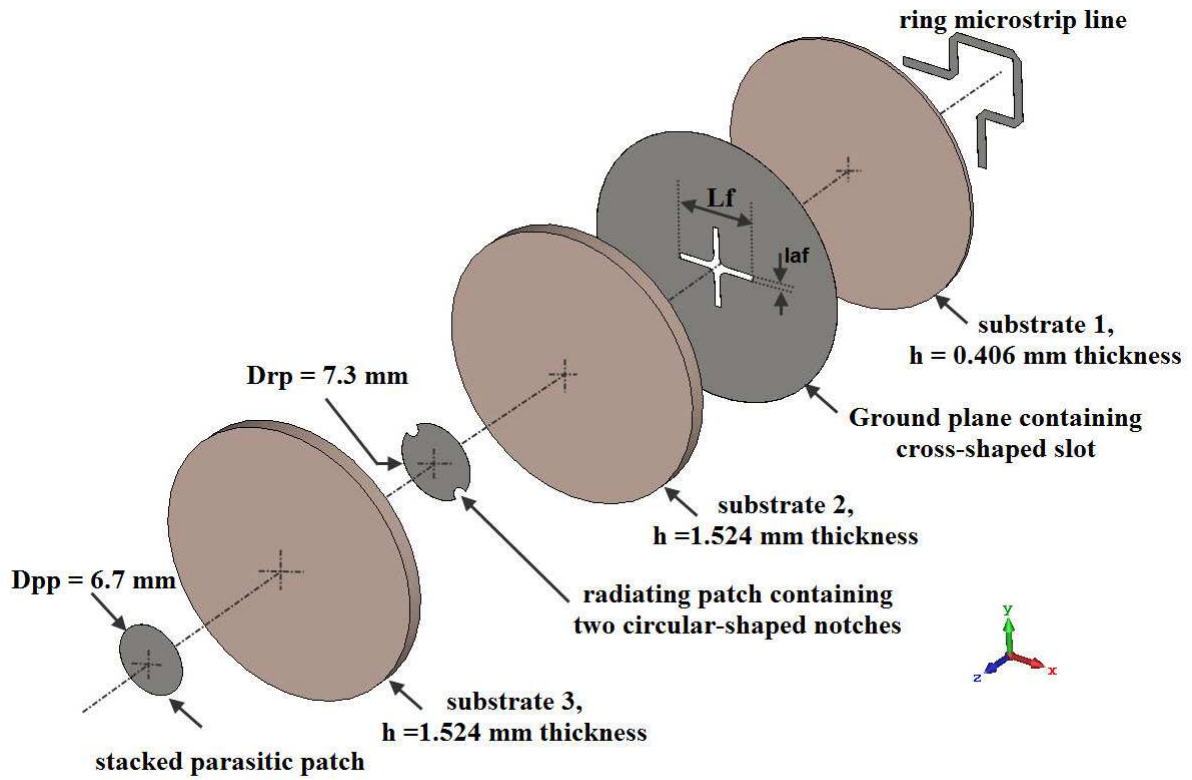


Fig. 3. Exploded view showing individual layers of the DCPFF.

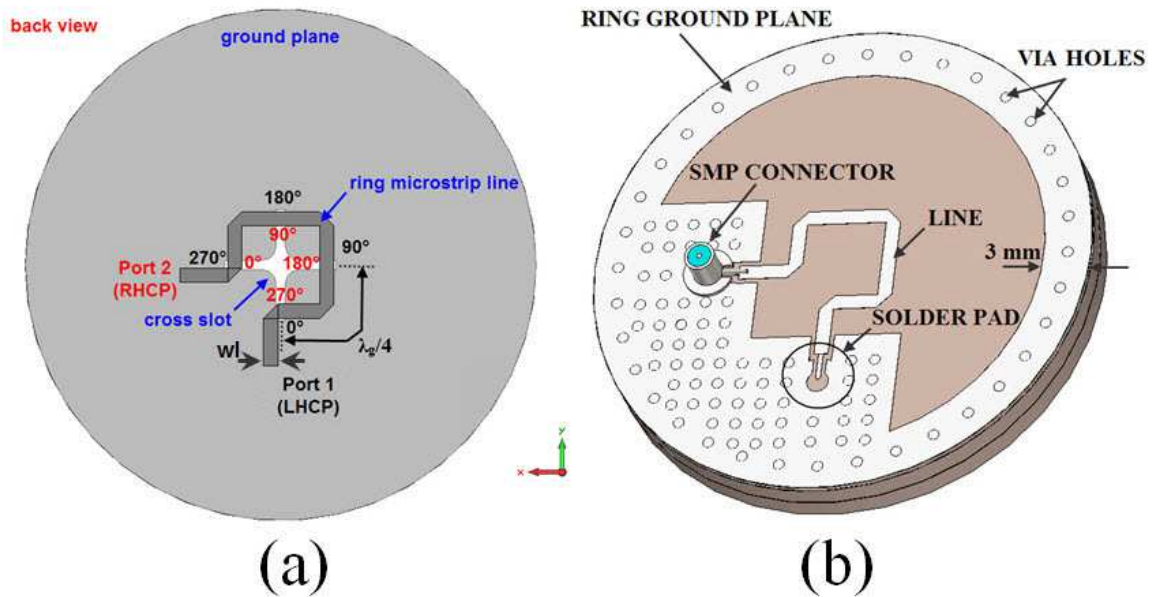


Fig. 4. Ring microstrip. (a) Sequential phase feed. (b) Realization

IV. Measurement and simulation validation

A) Realized structure

1) DCPFF realization

Fig. 4.b shows the DCPFF realization (back view). Two SMP-M type coaxial connectors are soldered to each input of the 50Ω microstrip line. An adapter SMP-F to SMA-F is connected during measurement. A ring ground plane and via holes are realized to improve the electrical continuity between the 3U platform, the ground plane and the transition SMP/microstrip line. The three printed circuits have been realized in our laboratory with a Circuit Board Plotter and have been assembled by Loctite glue. This last one and the adapters are not taken into account in the simulation. This etching method often involves a substrate thickness decrease where the metallization is removed (in our cases, 1.48 mm instead 1.524 mm for substrates 2 and 3). A retro-simulation was made to take into account all these remarks without optimizing again some parameters such as the slot length.

2) Manufactured DCPIA

Fig. 5 (a-d) shows the manufactured DCPIA. An aluminium thin sheet allows simulating the 3U platform and reducing the interferences of the antenna test range interface.

B) Comparison between measurements and simulations

1) Return loss and isolation

Fig. 6.a presents the simulated and measured return loss of the two ports. The experimental return loss of each port is higher than the predicted one. This discrepancy is probably due to the SMP connectors soldering. However, this level is below -19 dB over a 400 MHz bandwidth. Fig. 6.b shows the isolation between the ports. A -12 dB isolation is almost obtained between 8.0-8.4 GHz. This isolation is below -20 dB between 8.15-8.35 GHz.

1) Directivity, realized gain and total efficiency

Fig. 7.a shows the comparison between the simulated and the measured directivity and maximum realized gain for the port 1. A satisfactory agreement is observed between these two results. It is the same for the port 2 (Fig. 7.b). A slight discrepancy appears which probably results from a 50 MHz frequency shift of the isolation and the SMP/SMA adapter losses. Fig. 8 shows that the total efficiency of DCPIA is identical to the feed one despite the presence of the horn. Excellent numerical results have been obtained with a total efficiency upper than 90% on the 8.0-8.4 GHz frequency band. The total efficiency measurement would have been close to 90% if no frequency shift appears in the isolation.

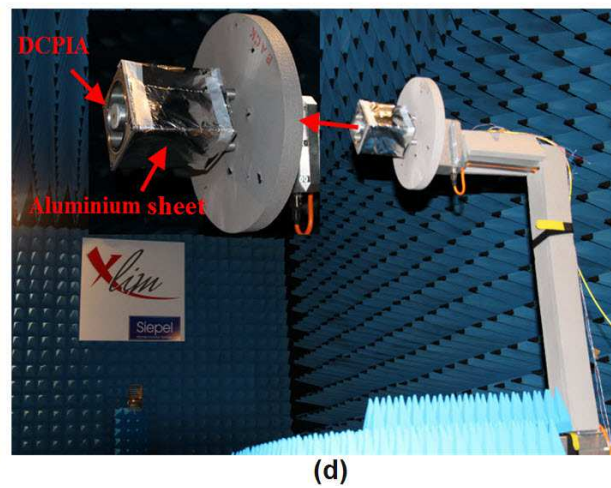
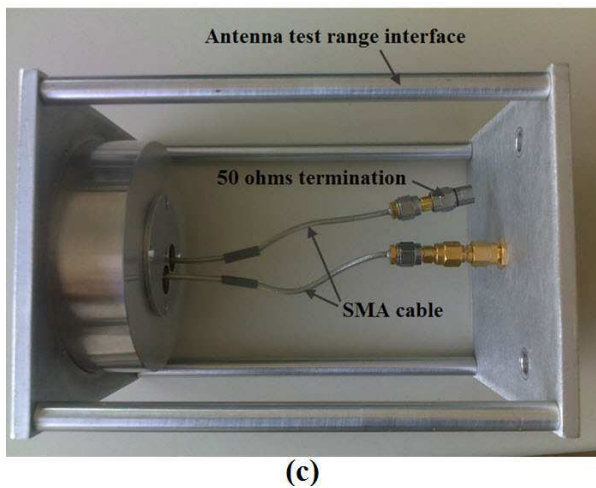
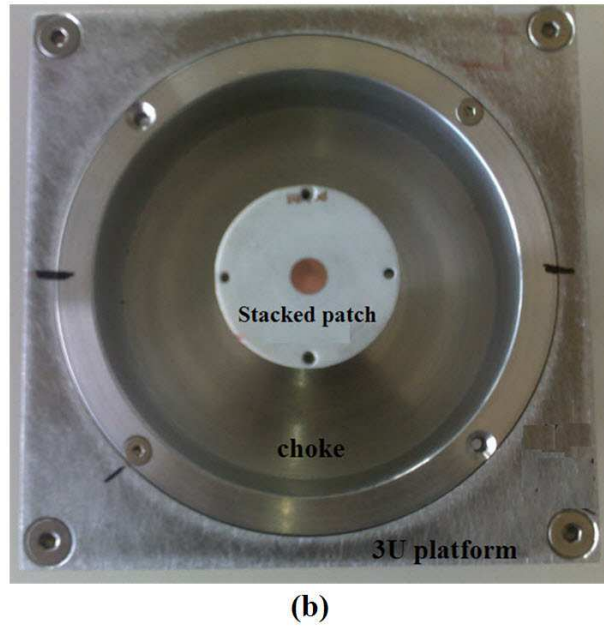
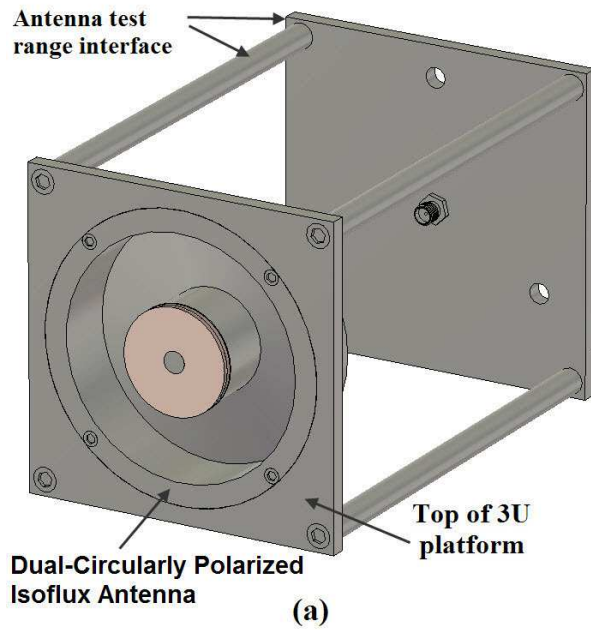


Fig. 5. Ring Manufactured DCPIA. (a) Drawing perspective view. (b) Top view photography. (c) Left view photography. (d) Photography of the DCPIA positioned on our antenna test range support

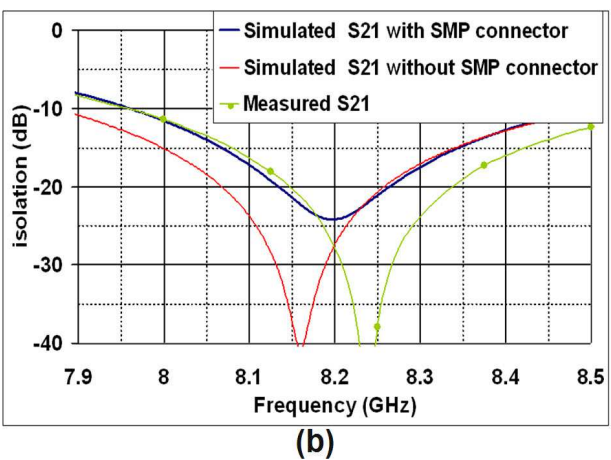
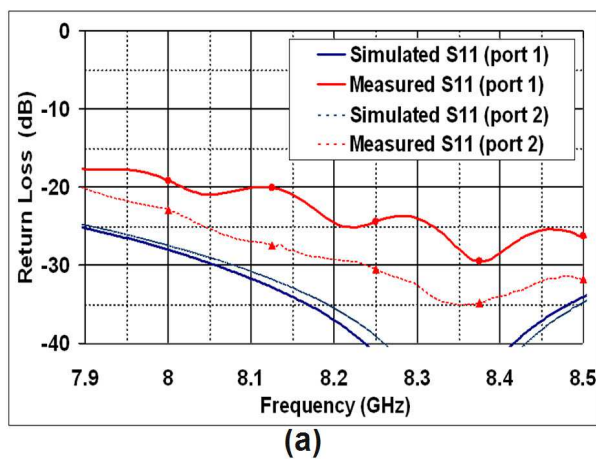


Fig. 6. [S] parameters. (a) Return loss. (b) Isolation

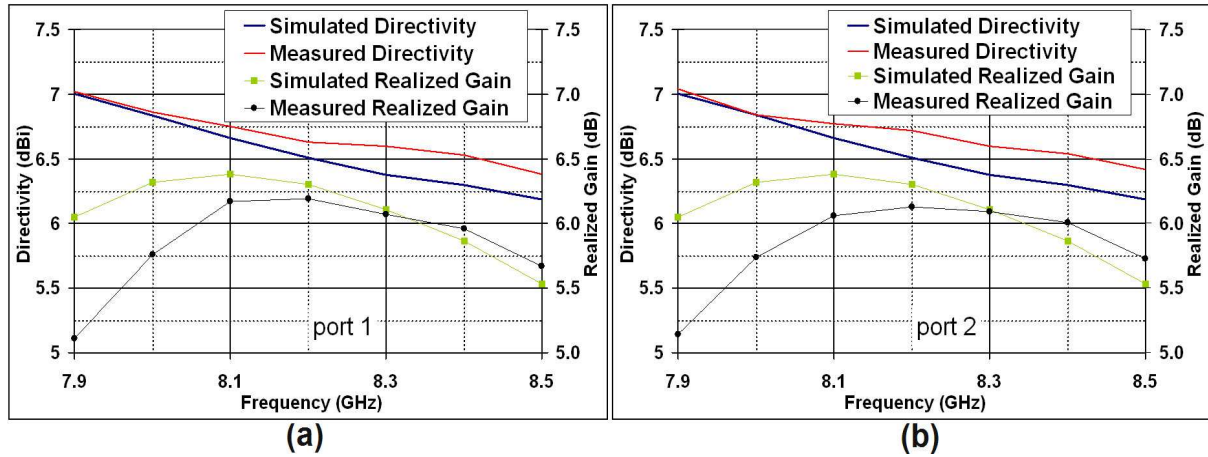


Fig. 7. (a) Directivity and Maximum realized gain of port 1. (b) Directivity and Maximum realized gain of port 2

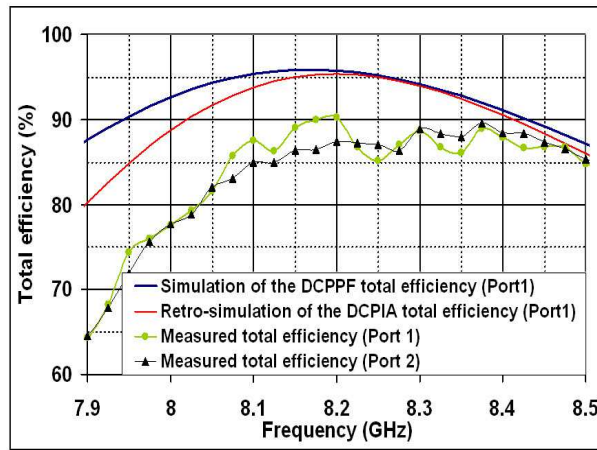


Fig. 8. Simulated and measured total efficiency

2) Radiation pattern and AR

Fig. 9 (a-b) show the comparison of the simulated and measured RHCP and LHCP radiation patterns of the port 1 and 2 at the central frequency (8.2 GHz) (RG drawn in the $\varphi = 0^\circ$ cut-plane). An isoflux shape is obtained on the frequency band but the RG is maximum at the $\theta_{gm} = 35^\circ$ angle instead of 65° . This was the same for the antenna studied in [1]. The RG is close to 0 dB whatever the azimuth angle (φ) and the port.

The measured AR radiation patterns (plane $\varphi = 0^\circ$) and AR at $\theta = 65^\circ$ versus azimuth angle (φ) are close to the simulated ones Fig. 10 (a-b). This characteristic almost meets to the antenna targets. This result would have been almost the same with other cut planes or frequencies.

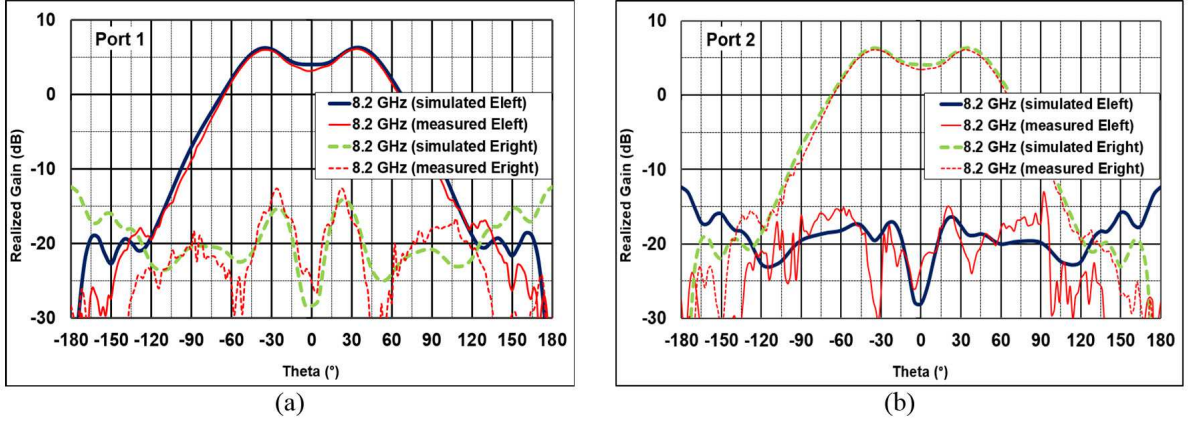


Fig. 9. LHCP and RHCP Radiation patterns ($\varphi = 0^\circ$ plane). (a) Simulation and measurement of port 1. (b) Simulation and measurement of port 2.

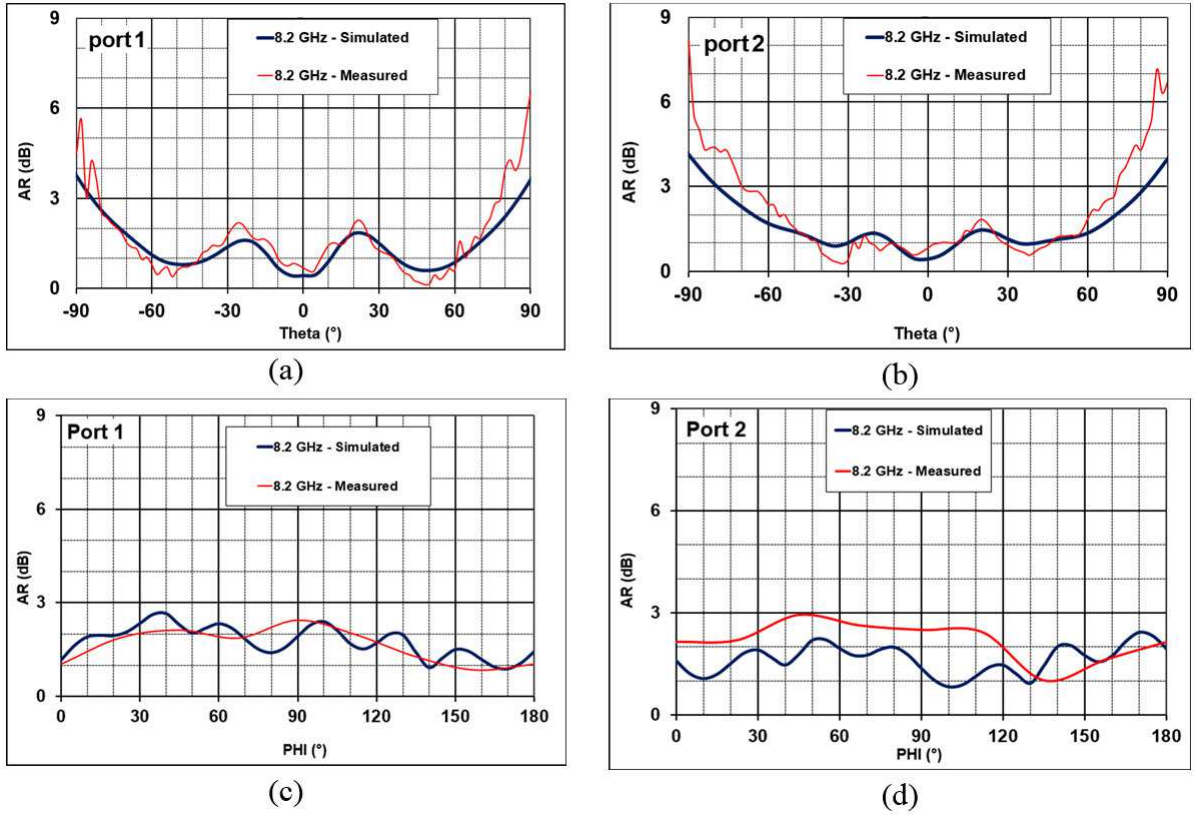


Fig. 10. LHCP AR patterns ($\varphi = 0^\circ$ plane). (a) port 1. (b) port 2. AR at $\theta = 65^\circ$ versus azimuth angle. (c) port 1. (d) port 2

The table II presents a comparison of measured and simulated antenna performances. All the specifications are obtained except the isolation and the LOC.

V. CONCLUSION

This paper completes the previous work on circularly polarized isoflux antenna for nanosatellite applications. The proposed design allows a dual circular polarization of this antenna. A very good agreement between simulation and measurement is obtained even if the

-20 dB desired isolation is not satisfied in all bandwidth (2.4 % instead 5%). The result can be improved by increasing the patch substrate thickness and by reducing the dielectric constant as shown in paper [29].

TABLE II: COMPARISON OF ANTENNA PERFORMANCES

Parameter	specification		
	target	simulation	measurement
Frequency band (GHz)	8.0 - 8.4	8.0 - 8.4	8.0 - 8.4
Return loss (dB)	< -20	< -20	< -19
Isolation between ports (dB)	< -20	< -12	< -11
Polarization	RHCP and LHCP	RHCP and LHCP	RHCP and LHCP
Limit of coverage (LOC)	65°	35°	35°
Minimum gain at LOC (dB)	0	> 0	> 0
Pattern shape	Isoflux pattern	Isoflux pattern	Isoflux pattern
Maximum AR(dB) at LOC	3	< 3	< 3

REFERENCES

- [1] Arnaud, L. Duchesne, K. Elis, J. Fouany, T. Monediere, M. Thevenot, "X-band compact choke horn antenna with circular polarization and isoflux pattern for nanosatellite applications", *International Journal of Microwave and Wireless Technologies*, April 2015. doi :10.1017/S1759078715000677
- [2] E. Arnaud, L. Duchesne, K. Elis, J. Fouany, T. Monediere, M. Thevenot, "Total efficiency enhancement of X-band compact choke horn antenna with circular polarization and isoflux pattern", *International Journal of Microwave and Wireless Technologies*, June 2015. doi : 10.1017/s1759078715001117
- [3] Fouany, J.; Thevenot, M.; Arnaud, E.; Torres, F.; Monediere, T.; Adnet, N.; Manrique, R.; Duchesne, L.; Baracco, J.M.; Elis, K., "Circularly polarized isoflux compact X band antenna for nano-satellites applications," in *Microwave Conference (EuMC), 2015 European*, vol., no., pp.1403-1406, 7-10 Sept. 2015doi: 10.1109/EuMC.2015.7346035
- [4] H. Geyer, "Runder Hornstrahler mit ringformigen Sperrtopfen zur gleichzeitigen Übertragung zweier polarisationsentkoppelter Wellen", *Frequenz*, 1966, 20, pp. 22-28 (especially p. 27)
- [5] A. LaGrone, G. Roberts, "Minor lobe suppression in a rectangular horn antenna through the utilization of a high impedance choke flange," *Antennas and Propagation, IEEE Transactions on*, vol.14, no.1, pp.102,104, Jan 1966, doi: 10.1109/TAP.1966.1138627
- [6] R. Wohlleben, H. Mattes, O. Lochner, "Simple small primary feed for large opening angles and high aperture efficiency," *Electronics Letters*, vol.8, no.19, pp.474,476, September 21 1972, doi: 10.1049/el:19720341
- [7] L. Shafai, "Broadening of primary feed patterns by small E-plane slots," *Electronics Letters*, vol.13, no.4, pp.102-103, February 17 1977.

- [8] P. Brachat, "Sectoral pattern synthesis with primary feeds," *Antennas and Propagation, IEEE Transactions on*, vol.42, no.4, pp.484-491, Apr 1994. doi: 10.1109/8.286216
- [9] D. Davis, O. Digiondomenico, J. Kempic., "A new type of circularly polarized antenna element", *Antennas and Propagation Society International Symposium*, Oct 1967
- [10] J. L. Cano, A. Tribak, R. Hoyland, A. Mediavilla, E. Artal, "Full band waveguide turnstile junction orthomode transducer with phase matched outputs", *Int J RF and Microwave Comp Aid Eng*, 20: 333–341, 2010. doi: 10.1002/mmce.20437
- [11] A. R. Maldonado, M. A. Panduroa, C. del Rio Bociob, A. Mendez, "Design of concentric ring antenna array for a reconfigurable isoflux pattern". *Journal of Electromagnetic Waves and Applications*, 2013 Vol. 27, No. 12, 1483–1495.
- [12] A. R. Maldonado, M. A. Panduroa, C. del Rio Bociob, A. Mendez, "Design of concentric ring antenna arrays for isoflux radiation in GEO satellites ". *Journal of IEICE Electronics Express* 2011, Vol. 8, No. 7, 484–490.
- [13] J. Jin, H. L. Wang, W. M. Zhu, and Y. Z. Liu, "Array Patterns Synthesizing Using Genetic Algorithm". *Progress In Electromagnetics Research Symposium 2006*, Cambridge, USA, March 26-29.
- [14] M. Ibarra, A. Reyna, M. A Panduro1, C. del Rio-Bocio, "Design of Aperiodic Planar Arrays for Desirable Isoflux Radiation in GEO Satellites", *Antennas and Propagation (APSURSI) 2011*, Spokane.
- [15] J. L. Araque Quijano, M. Righero, G. Vecchi, "Sparse 2D array placement for arbitrary pattern mask and with excitation constraints: a simple deterministic approach", *IEEE Transactions on Antenna and Propagation*, accepted 2013.
- [16] S. M. Roy, I. Balbin, "Handheld Reader Antenna at 5.8 GHz", Department of Electrical and Computer Systems Engineering, Monash University, Clayton, Victoria, Australia.
- [17] Kim Boyon, Pan Bo, S. Nikolaou, Kim Young-Sik, J. Papapolymerou, M. M. Tentzeris, "A Novel Single-Feed Circular Microstrip Antenna With Reconfigurable Polarization Capability," *Antennas and Propagation, IEEE Trans. on* , vol.56, no.3, pp.630,638, March 2008.
- [18] Keng-Hsien Chen; Jhao-Ru Chen; Sung-Jung Wu; Jenn-Hwan Tarn, "A multi-eared antenna with frequency and polarization reconfigurability," *Microwave Conference Proceedings (APMC), 2011 Asia-Pacific* , vol., no., pp.1314,1317, 5-8 Dec. 2011
- [19] Qin Pei-Yuan, A. R. Weily, Y. J. Guo, Liang Chang-Hong, "Polarization Reconfigurable U-Slot Patch Antenna," *Antennas and Propagation, IEEE Transactions on* , vol.58, no.10, pp.3383,3388, Oct. 2010, doi: 10.1109/TAP.2010.2055808
- [20] Wu Yi-Fan; Wu Chun-Hsien; D. Y. Lai, Chen Fu-Chiarng, "A Reconfigurable Quadri-Polarization Diversity Aperture-Coupled Patch Antenna," in *Antennas and Propagation, IEEE Transactions on* , vol.55, no.3, pp.1009-1012, March 2007, doi: 10.1109/TAP.2006.889947
- [21] A. Narbudowicz, B. Xiulong, M. J. Ammann, "Dual Circularly-Polarized Patch Antenna Using Even and Odd Feed-Line Modes," *Antennas and Propagation, IEEE Transactions on* , vol.61, no.9, pp.4828,4831, Sept. 2013, doi: 10.1109/TAP.2013.2269471
- [22] Li Yue; Zhang Zhijun; Chen Wenhua; Feng Zhenghe; M. F. Iskander, "A Dual-Polarization Slot Antenna Using a Compact CPW Feeding Structure," *Antennas and Wireless Propagation Letters, IEEE*, vol.9, no., pp.191,194, 2010, doi: 10.1109/LAWP.2010.2044865
- [23] Lai Xiao-Zheng, Xie Ze-Ming, Xie Qi-Qiu; Cen Xuan-Liang, "A Dual Circularly Polarized RFID Reader Antenna With Wideband Isolation," *Antennas and Wireless*

Propagation Letters, IEEE, vol.12, no., pp.1630,1633, 2013, doi: 10.1109/LAWP.2013.2294173

- [24] A. K. Sharma, A. Mittal, "Diagonal slotted diamond shaped dual circularly polarized microstrip "patch" antenna with dumbbell aperture coupling," Microwave Conference, 2005 European , vol.3, no., pp.3 pp., 4-6 Oct. 2005, doi: 10.1109/EUMC.2005.1610326
- [25] Zhu Wei, Xiao Shaoqiu, Yuan Rui, Tang Mingchun, "Broadband and dual circularly polarized "patch" antenna with H-shaped aperture," Antennas and Propagation (ISAP), International Symposium on , vol., no., pp.549,550, 2-5 Dec. 2014, doi: 10.1109/ISANP.2014.7026769
- [26] Xudong Bai , Xianling Liang , Li Minzhu, Zhou Bin, Jin Junping Geng, Ronghong, "Dual-Circularly Polarized Conical-Beam Microstrip Antenna," Antennas and Wireless Propagation Letters, IEEE , vol.14, no., pp.482,485, 2015, doi: 10.1109/LAWP.2014.2369515
- [27] E. Aloni, R. Kastner, "Analysis of a dual circularly polarized microstrip antenna fed by crossed slots," in Antennas and Propagation, IEEE Transactions on , vol.42, no.8, pp.1053-1058, Aug 1994
- [28] M. T. Zhang, Y. B. Chen, Y. C. Jiao & F. S. Zhang (2006), "Dual Circularly Polarized Antenna of Compact Structure for RFID Application, Journal of Electromagnetic Waves and Applications, 20:14, 1895-1902, DOI:10.1163/156939306779322611
- [29] Changhong Zhang, Junping Geng, Bin Zhou, Xianling Liang, and Ronghong Jin, "A Broadband Single-Feed Circularly Polarized Patch Antenna with Wide Beamwidth," International Journal of Antennas and Propagation, Article ID 740274, 10 pages, 2015



Eric Arnaud was born in France in 1970. He received the Diplôme D'Etudes Supérieures Spécialisées (DESS) and Ph.D. degrees in Electronics and Telecommunication from the University of LIMOGES in 1994 and 2010, respectively. He did his Ph.D. on circularly polarized EBG antenna. From 1996 to 2001, he has been in charge of the Microwave part of Free-Electron Laser (L.U.R.E). Since 2001, he has been in charge of XLIM laboratory's antenna test range. He participated in several research projects related to the design, development and characterization of antennas. His research interests are mainly in the fields of circularly polarized EBG antenna, agile electromagnetic band gap matrix antenna and isoflux pattern antenna.



Cyrille Menudier was born in France, in 1981. He received the MSc in High-Frequency Telecommunications from the University of Limoges and the Engineer degree from ENSIL in Electronics in 2004. He received his PhD in Telecommunications from the XLIM Research Laboratory, University of Limoges, in 2007. He then got a post-doctoral position in CNES (French Space Agency), Toulouse, until 2009, where he worked on reconfigurable reflectarray antennas. He is currently an Associate Professor in the *Antennas & Signal Team – RF Systems Axis* of the XLIM Research Laboratory. His research interests include reconfigurable antennas, phased arrays, reflectarrays, parasitic element antennas and mutual coupling effects.



Jamil Fouany: was born in Lebanon, in 1989. He received the Master's degree in electronic and optical engineering for high frequency communications (IXEO) from the University of Limoges, France in 2012. He is currently toward the Ph.D. degree in High Frequency Communications, photonics and systems in the XLIM Laboratory, University of Limoges. His research interests include parasitic antennas with circular polarization.



Thierry Monediere was born in 1964 in Tulle (France). He obtained his PhD in 1990 in the IRCOM Laboratory of the University of Limoges. He is actually the head of department "Waves and Associated Systems" of Xlim laboratory and Professor in the University of Limoges. He develops his research activities in Xlim Laboratory (UMR CNRS/University of Limoges). He works on multifunction antennas, EBG antennas and also active antennas.



Marc Thevenot was born in Limoges, France, in February 1971. He received the BS and M.Sc. degrees in Microwaves from the University of Limoges, France, in 1995. He received the Ph.D. Degree in Electronic from the University of Limoges in 1999. He joined the CNRS in 2001. He is responsible of multifunction antennas activities in the "Waves and Associated Systems" department of Xlim. His main current research activities deal with the electromagnetism, EBG antennas, materials, parasitic element antennas, reconfigurable antennas and reflectarray antennas.

List of figures and tables

Fig. 11. Definition of the compact choke horn antenna

Fig. 12. DCPIA mechanical assembly

Fig. 13. Exploded view showing individual layers of the DCPPF

Fig. 14. Ring microstrip. (a) Sequential phase feed. (b) Realization

Fig. 15. Ring Manufactured DCPIA. (a) Drawing perspective view. (b) Top view photography. (c) Left view photography. (d) Photography of the DCPIA positioned on our antenna test range support

Fig. 16. [S] parameters. (a) Return loss. (b) Isolation

Fig. 17. (a) Directivity and Maximum realized gain of port 1. (b) Directivity and Maximum realized gain of port 2

Fig. 18. Simulated and measured total efficiency

Fig. 19. LHCP and RHCP Radiation patterns ($\varphi = 0^\circ$ plane). (a) Simulation and measurement of port 1. (b) Simulation and measurement of port 2

Fig. 20. LHCP AR patterns ($\varphi = 0^\circ$ plane). (a) port 1. (b) port 2. AR at $\theta = 65^\circ$ versus azimuth angle. (c) port 1. (d) port 2

Table I: Antenna performances target

Table II: Comparison of Antenna performances